



Degradation of Orange G dye by hexacyanoferrate(III) ions in the presence of Iridium nanoparticles: effect of system parameters and kinetic study

Anjali Goel*, Rajni Lasyal

Department of Chemistry, Kanya Gurukul Campus, Gurukul Kangri University, Haridwar, Uttarakhand 249407, India, Tel. +91 9412942338; email: anjaligoel10@gmail.com (A. Goel), Tel. +91 9634461412; email: lasyal.rajni@gmail.com (R. Lasyal)

Received 12 February 2015; Accepted 13 August 2015

ABSTRACT

The kinetics of the catalytic degradation of Orange G (OG), an azo dye containing two sulphonic groups, by hexacyanoferrate(III) ions (HCF(III)) in the presence of iridium nanoparticles (Ir nano) has been investigated. The effect of various operational parameters such as the concentration of dye, oxidant, catalyst and solution pH on the reaction rate have been determined. The results show that the reaction follows first-order kinetics with respect to [HCF(III)] at optimum pH 8.0 and constant temperature of $40 \pm 0.1^\circ\text{C}$. The order of reaction with respect to [OG] has been found to be one at its lower concentration tending towards zero at its higher concentration. The reaction rate increases with an increase in the concentration of iridium nanoparticles used as catalyst which reveals the good catalytic activity of Ir nano. Thermodynamic parameters have been calculated by studying the reaction rate at four different temperatures. Based on the experimental results, a plausible reaction mechanism involving complex formation and rate law has been derived. The UV-vis, FT-IR, HPLC, LC-MS of degradation product showed the formation of simpler and less hazardous compound, 6-hydroxyamino benzene-1,2-diethanoic acid, 6-hydroxyamino benzene-1,2-diethanoic anhydride and 7-hydroxy naphthalene-1,3-disulphonic acid as minor degradation products and pentanoic acid, propanoic acid, ethanoic acid as major degradation products.

Keywords: Kinetics; Degradation; Orange G; HCF(III); Ir nanoparticles

1. Introduction

Environmental pollution on global scale has drawn much attention to the need for developing ecologically clean chemical technology, materials and processes [1]. Textile dyes constitute one of the largest groups of organic compounds that represent an increasing environmental concern with reference to water pollution [2]. Azo dyes with one or more azo group (N=N) being the largest and most diverse group of synthetic

dyes, constitute up to 70% of all the known commercial dyes produced [3]. They are widely used in various industries, such as those producing textiles, foods, cosmetics and paper printing [4]. Low reactivity of the azo linkage makes this class of compounds resistant to degradation [5]. These dyes not only impart colours to water sources but also damage living organisms by stopping the reoxygenation capacity of water, blocking sunlight, and therefore disturbing the natural growth activity of aquatic life. Thus, the removal of azo dyes from textile wastewater is a major environmental

*Corresponding author.

concern. Many techniques, such as activated carbon adsorption, flocculation, electrocoagulation, UV light degradation and redox treatments are being routinely used for azo dye degradation [6–10]. However, due to the ineffectiveness of these techniques in some way or other, the present scenario requires better and improved wastewater treatment measures.

Recently, nanotechnology has been extended to wastewater treatments [11,12]. Noble metal nanoparticles with high specific catalytic activity are ubiquitous in modern synthetic organic chemistry during the recent decades [13]. In this study, synthesized colloidal dispersion of iridium nanoclusters are used as catalyst in the oxidation of Orange G (OG), an azo dye, by hexacyanoferrate(III) in aqueous alkaline media. Goel and Sharma have used this technique in the oxidation of some amino acids [14,15] and mono azo dyes such as methyl orange [16] and orange II [17] containing one sulphonic group. In the present work, the purpose is to study the oxidative degradation of OG, a mono azo dye with two sulphonic groups. The oxidative degradation with respect to some important operating parameters such as pH of solution, [HCF(III)], [Ir nano], [OG] and temperature have been investigated to provide more.

2. Experimental

2.1. Materials

All the chemicals and reagents used were of AR grade. OG was procured from SRL (Sisco Research Laboratories Pvt. Ltd, India). The structure of an azo dye is shown in Fig. 1. pH of the reaction mixture was maintained using KH_2PO_4 and NaOH as buffer. Ir nano (particle size 4 nm) were synthesized by wet reduction method using polyvinylpyrrolidone as protecting agent after the reduction of precursor salt, $\text{IrCl}_3 \cdot 3\text{H}_2\text{O}$, by methanol as reported earlier [18].

2.2. Experimental procedures

The kinetic experiments were carried out at optimum pH (8.0) and constant temperature ($40 \pm 0.1^\circ\text{C}$). The requisite amount of each reactant was thermostated at 40°C to attain thermal equilibrium.

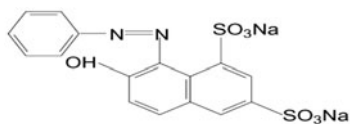


Fig. 1. Chemical Structure of the azo dye OG.

The appropriate quantities of reactants were mixed in a 100-ml iodine flask. The reaction was initiated by injecting the solution of OG into the aforementioned reaction mixture (prepared solution of HCF(III) and Ir nano). The progress of the reaction was measured spectrophotometrically (Systronics-117) with a spectrometric quartz cell (1 cm in path length) at 479 nm corresponding to the λ_{max} of the reaction mixture. It was verified that there is a negligible interference from other species present in the reaction mixture at this wavelength. As the reaction proceeds, the absorbance of the reaction mixture decreases with time and decrease in the absorbance of reaction mixture with time shows a linear relationship between dye concentration and absorbance. Initial rate of reaction rate was calculated from the slope of concentration vs. time curve according to constant—volume batch system mole balance equation $(dC_A/dt)_i = r_{\text{OG},i}$ where $r_{\text{OG},i}$ denotes the initial rate of degradation of dye.

2.3. Analytical methods

The reaction mixture was kept at atmospheric conditions for 24 h and the products were extracted with ethyl acetate. The degradation of dye and identification of degradation products were characterized by FT-IR (Bruker, Alpha E-FTIR), HPLC (SHIMADZU, LC-2010CHT) and LC-MS (BRUKER, ELITE). The mobile phase consisted of acetonitrile: water at (1:1) at the flow rate of 300 $\mu\text{L}/\text{min}$.

3. Results and discussion

3.1. Kinetic study

The oxidation kinetics of OG (both catalyzed and uncatalyzed reactions) has been studied at constant pH and temperature at different concentrations of one reactant keeping the concentration of others constant.

3.1.1. Effect of pH

The pH of the reaction mixture plays a significant role in the degradation of organic compounds. In the case of ionic reactions, the pH affects ionization and the optimum value is sought at which ionization is maximum and then the rate of reaction is measured at that optimum pH value. The effect of pH on the degradation of OG was studied by varying pH of solution from 6 to 9.5. Fig. 2 shows that the optimum pH for the degradation of OG is 8 indicating the maximum ionization. In alkaline medium, OH^- reacts with dye to extract proton and form anionic species, D^- in equilibrium [17]. At high pH values, the rate of

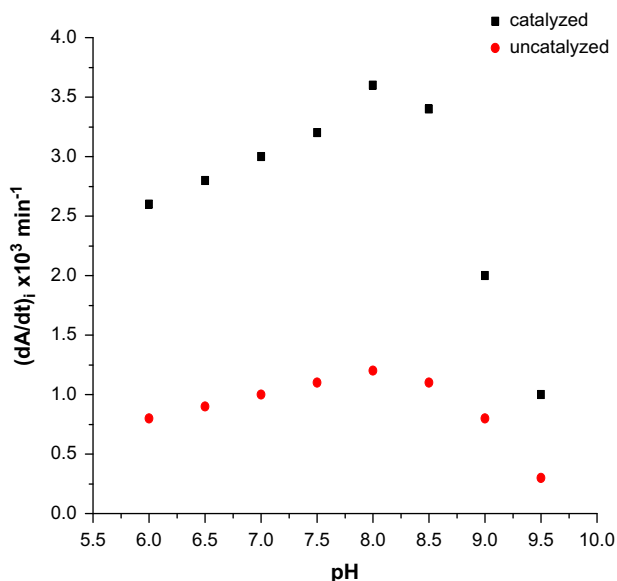


Fig. 2. Effect of pH on initial degradation rate of OG by [HCF(III)]. Experimental conditions: [OG] = 3.0×10^{-5} mol dm $^{-3}$; [HCF(III)] = 3.0×10^{-6} mol dm $^{-3}$; [Ir nano] = 1.004×10^{-7} mol dm $^{-3}$; temperature = 40 ± 0.1 °C.

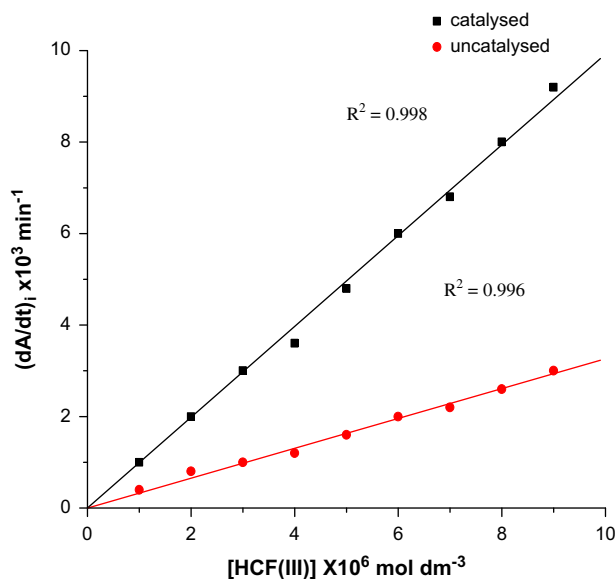


Fig. 3. Effect of [HCF(III)] on initial degradation rate of OG by [HCF(III)]. Experimental conditions: [OG] = 3.0×10^{-5} mol dm $^{-3}$; [Ir nano] = 1.004×10^{-7} mol dm $^{-3}$; pH 8.0; temperature = 40 ± 0.1 °C.

degradation may decline due to Coulombic repulsion between anionic dye surface and hydroxyl anion, hence do not have opportunity to react with dye molecules [19,20].



3.1.2. Effect of [HCF(III)]

The kinetic results presented in Fig. 3 show effect of oxidant's concentration on initial reaction rate. The oxidation of OG follows first-order kinetics with respect to [HCF(III)]. The concentration of HCF(III) was varied from 1×10^{-6} to 9×10^{-6} mol dm $^{-3}$.

3.1.3. Effect of [OG]

The effect of substrate concentration on initial reaction rate was studied by varying its concentration from 1×10^{-5} to 9×10^{-5} mol dm $^{-3}$. The data presented in Fig. 4 show first-order dependence of rate on lower concentration of substrate which tends to be zero order at its higher concentration.

3.1.4. Effect of [catalyst]

A gradual increase in rate with Ir nano concentration reveals first-order kinetics with respect to

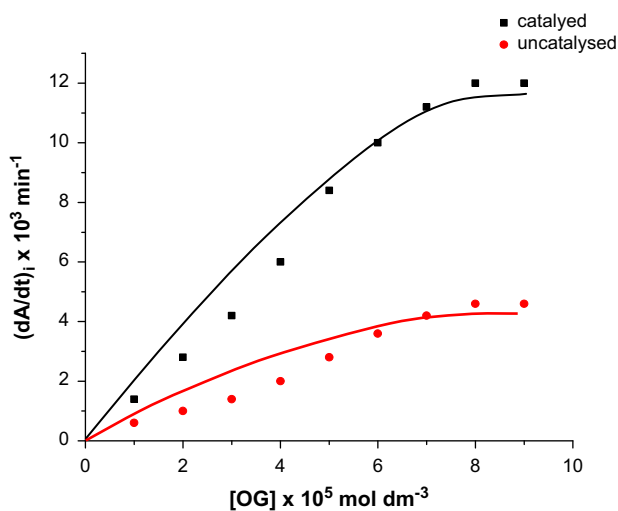


Fig. 4. Effect of [OG] on initial degradation rate of OG by [HCF(III)]. Experimental conditions: [HCF(III)] = 3.0×10^{-6} mol dm $^{-3}$; [Ir nano] = 1.004×10^{-7} mol dm $^{-3}$; pH 8.0; temperature = 40 ± 0.1 °C.

[Ir nano] (Fig. 5). The concentration of Ir nanoparticles was varied about many times from 0.2×10^{-7} to 1.204×10^{-7} mol dm $^{-3}$. The rate of reaction varied with the amount of catalyst, this means that the rate of reaction may have been controlled by the mass of catalyst.

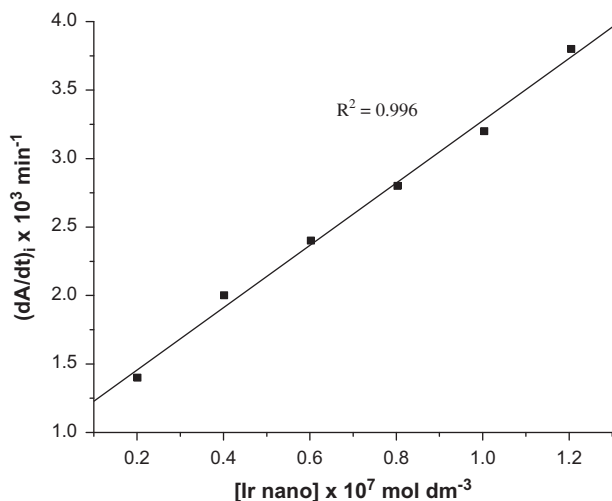


Fig. 5. Effect of [Ir nano] on initial degradation rate by [HCF(III)]. Experimental conditions: [OG] = 3.0×10^{-5} mol dm $^{-3}$; [HCF(III)] = 3.0×10^{-6} mol dm $^{-3}$; pH 8.0; temperature = 40 ± 0.1 °C.

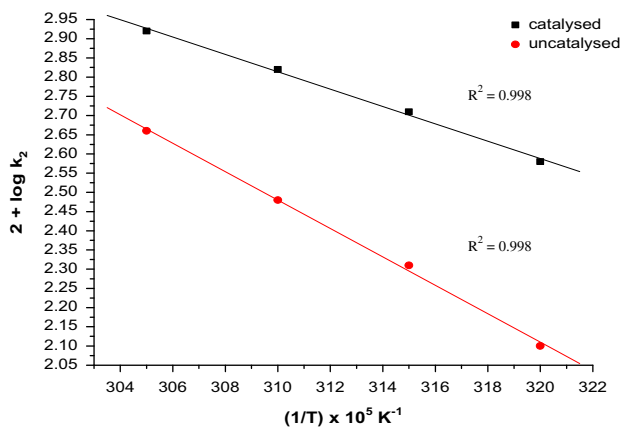


Fig. 6. Arrhenius plot for initial degradation rate of OG by [HCF(III)]. Experimental conditions: [OG] = 3.0×10^{-5} mol dm $^{-3}$; [HCF(III)] = 3.0×10^{-5} mol dm $^{-6}$; [Ir nano] = 1.004×10^{-7} mol dm $^{-3}$; pH 8.0.

3.1.5. Thermodynamic parameters

The thermodynamic parameters for both catalyzed and uncatalyzed reactions have been evaluated by studying the reaction at four different temperatures, i.e. 40, 45, 50 and 55 °C (Table 1). The rate of a reaction depends on the temperature according to Arrhenius equation:

$$k = Ae^{-Ea/RT} \quad (2)$$

Activation parameters, Ea and Arrhenius factor (A) were evaluated from Arrhenius plots (Fig. 6). Enthalpy

Table 1

Thermodynamic parameters

Parameter	Values	
	(Uncatalysed)	(Catalyzed)
k_2 (l mol $^{-1}$ min $^{-1}$)	2.74	5.96
Ea (kcal mol $^{-1}$)	17.48	10.50
ΔH^\ddagger (kcal mol $^{-1}$)	16.852	9.86
ΔS^\ddagger (eu)	-4.54	-24.44
ΔF^\ddagger (kcal mol $^{-1}$)	18.29	17.69
A (l mol $^{-1}$ sec $^{-1}$)	2.08×10^{12}	8.29×10^7

of activation (ΔH^\ddagger), entropy of activation (ΔS^\ddagger) and energy of formation (ΔF^\ddagger) were calculated from Eqs. (3)–(5), respectively:

$$\Delta H^\ddagger = Ea - RT \quad (3)$$

$$k_r = (kT/h)e^{\Delta S^\ddagger/R}e^{-\Delta Ea/RT} \quad (4)$$

$$\Delta F^\ddagger = \Delta H^\ddagger - T\Delta S^\ddagger \quad (5)$$

The data reveals low energy of activation for catalyzed reaction as compared to uncatalyzed reaction. It reveals good catalytic activity of Ir nano. Large negative entropy of activation for catalyzed reaction shows more disorderness amongst the reactants and the formation of polar species during the reaction. Energy of formation is almost same for both the catalyzed and uncatalyzed reactions suggesting similar mechanism involved during the reaction. Comparison of the data with previously reported oxidation of methyl orange and orange II shows that the rate of degradation of OG is slower than that of methyl orange [16] and orange II [17] which may be attributed to the presence of two sulphonic groups. The sulphonic groups present in dyes leads to the formation of sulphate ions which decrease the extent of further degradation and thus decreases the rate [21]. Thus, more is the number of sulphonic groups attached to

Table 2

Rate of degradation of reaction mixture for three consecutive cycles

No. of cycles	$(-dA/dt)_i \times 10^3$ (min $^{-1}$)
Before recovery	3.0
After I cycle	2.6
After II cycle	2.2
After III cycle	2.0

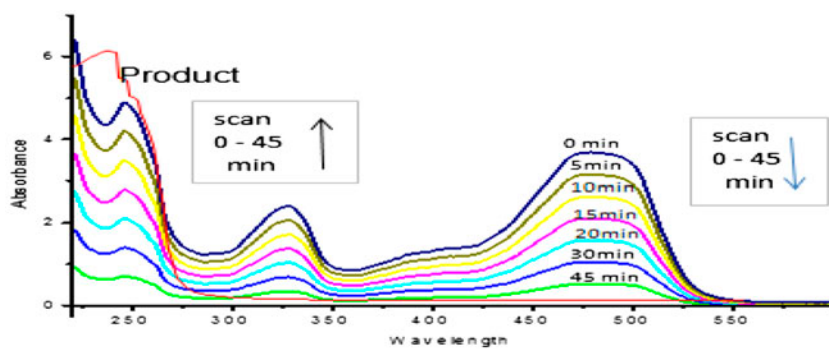


Fig. 7. UV-vis spectra showing the degradation of OG.

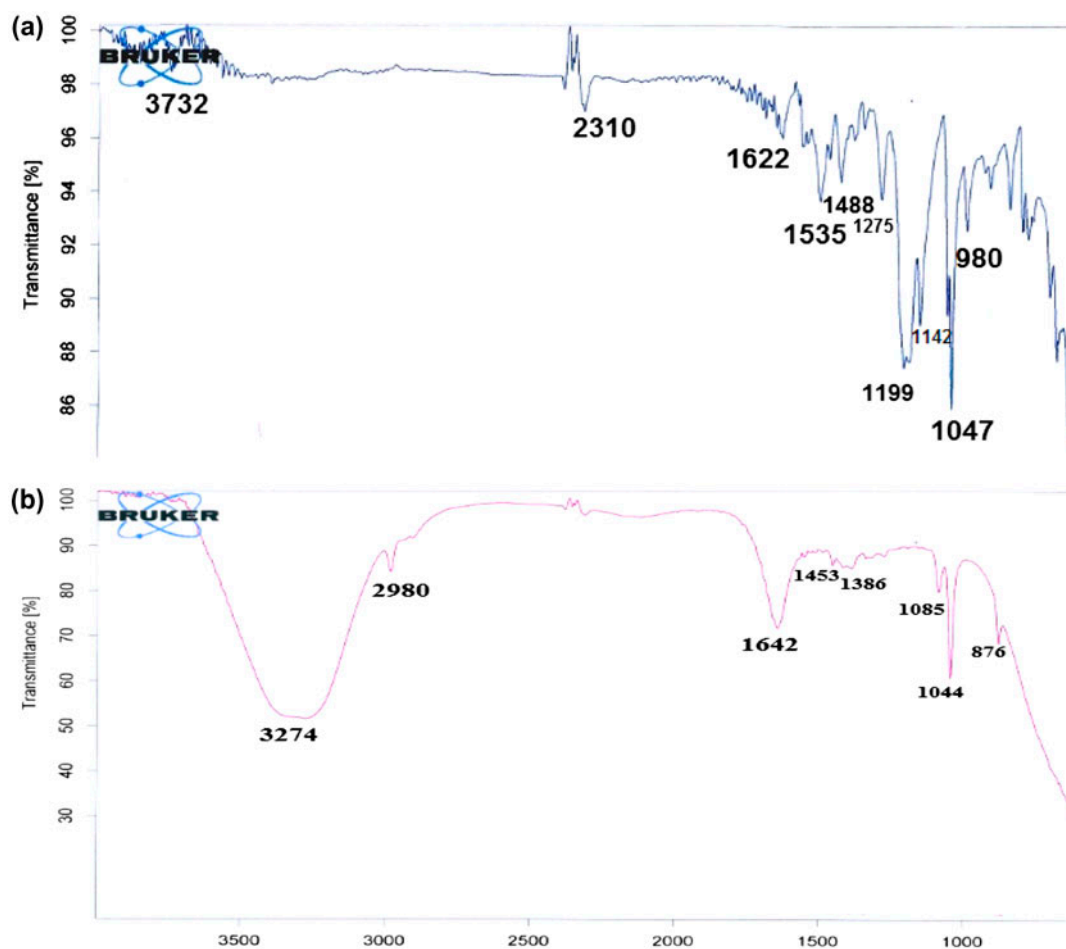


Fig. 8. FT-IR of (a) OG and (b) degradation product.

the dye, lesser is the degradation. The almost same value of energy of formation suggest that the mechanism involved is same as that for methyl orange and orange II.

3.1.6. Efficiency of recycled catalyst

In order to investigate the economy of the present method, Ir nanoparticles were recovered and reused

for three consecutive cycles. After the first degradation cycle, the treated reaction mixture was centrifuged. The obtained nanoparticles were washed thoroughly with double-distilled water five to six times and were further reused as catalyst in the kinetic study. The same method was used for three successive cycles at fixed experimental conditions. The results are presented in Table 2. It was found that the rate of reaction decreased with each successive cycle. This may be due to the increase in size of nanoparticles due to agglomeration.

3.2. Product analysis

Successful degradation of an azo dye, OG by HCF (III) ions in the presence of Ir nanoparticles has been confirmed by UV–vis spectrum as shown in Fig. 7. The spectrum corresponds to the disappearance of peak at 479 nm and the appearance of a new peak at 241 nm suggesting the formation of new product/products. The FT-IR analysis of OG and product also confirm the degradation. The FT-IR of OG displays bands at 3,732, 2,310, 1,622, 1,535, 1,488, 1,275, 1,199, 1,142, 1,047 and 980 cm^{-1} . The comparison of FT-IR spectra of OG and degradation product (Fig. 8) shows the disappearance of the band characteristic of azo bond at 1,488 cm^{-1} of OG in the spectra of product indicating the degradation of dye and the appearance

of new bands at 3,274 for OH stretching, 2,980 (CH_3 stretching), 1,642 ($\text{C}=\text{O}$ stretching), 1,044, 1,085 and, 876 cm^{-1} which are attributed to the formation of some new compounds [22,23].

Comparative study of HPLC chromatogram of OG and degradation products as given in Fig. 9 suggests the formation of new compounds. Fig. 9(b) shows three major peaks at 4.0, 10.6, 16.7 min and four minor peaks at 2.7, 7.8, 9.2, 24.1 min which are completely different from that of OG in Fig. 9(a) with one major peak at 1.4 min. LC–MS of extracted product/products is given in Fig. 10 indicating the formation of anticipated 6-hydroxyamino benzene-1,2-diethanoic acid, 6-hydroxyamino benzene-1,2-diethanoic anhydride and 7-hydroxy naphthalene-1,3-disulphonic acid as minor degradation products and pentanoic acid, propanoic acid, ethanoic acid as major degradation products which are simple and less hazardous (Table 3).

3.3. Mechanism

Based on the above experimental results and previously reported work, the following reaction mechanism for the oxidation of OG can be proposed:

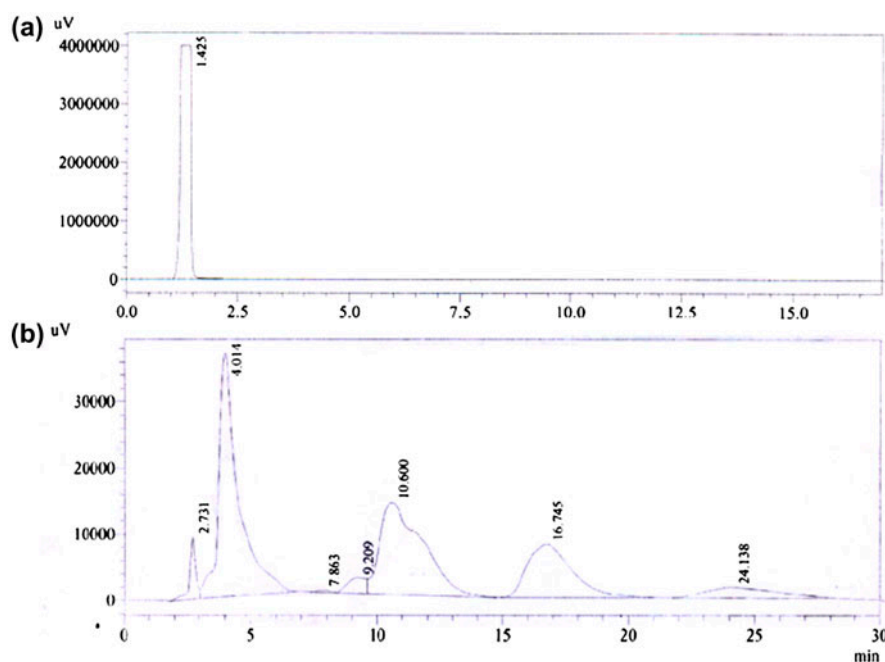
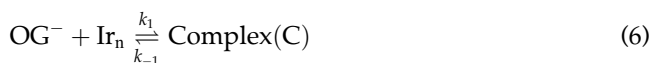
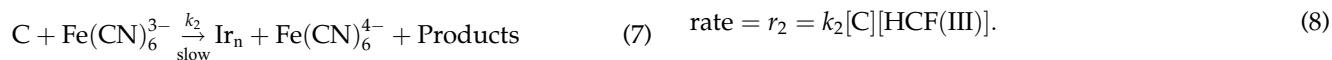


Fig. 9. (a) HPLC chromatogram of OG and (b) degradation products of OG.



In the above scheme, it is assumed that in alkaline medium mono azo dye OG exist as anion (OG^-) [24] which slowly forms a loosely bonded complex with iridium nanoparticles (Ir_n). This complex (C) slowly reacts with $\text{HCF}(\text{III})$ ion resulting into products along with Ir_n and $\text{Fe}(\text{CN})_6^{4-}$.

3.4. Rate law

From the above reaction mechanism, reaction rate will be:

During the reaction the $[\text{Ir}_n]_T$ (total iridium concentration) will be:

$$[\text{Ir}_n]_T = [\text{Ir}_n] + [\text{C}] \quad (9)$$

The complex formed in Eq. (6) is short lived. In Eq. (6), it is formed while in Eq. (7), it may decompose into final product. It is also possible that the complex may dissociate into Ir nano and dye anion. Thus, the overall concentration of complex in the reaction mixture remains constant. Hence, steady state treatment can be applied to its concentration. Thus, applying the

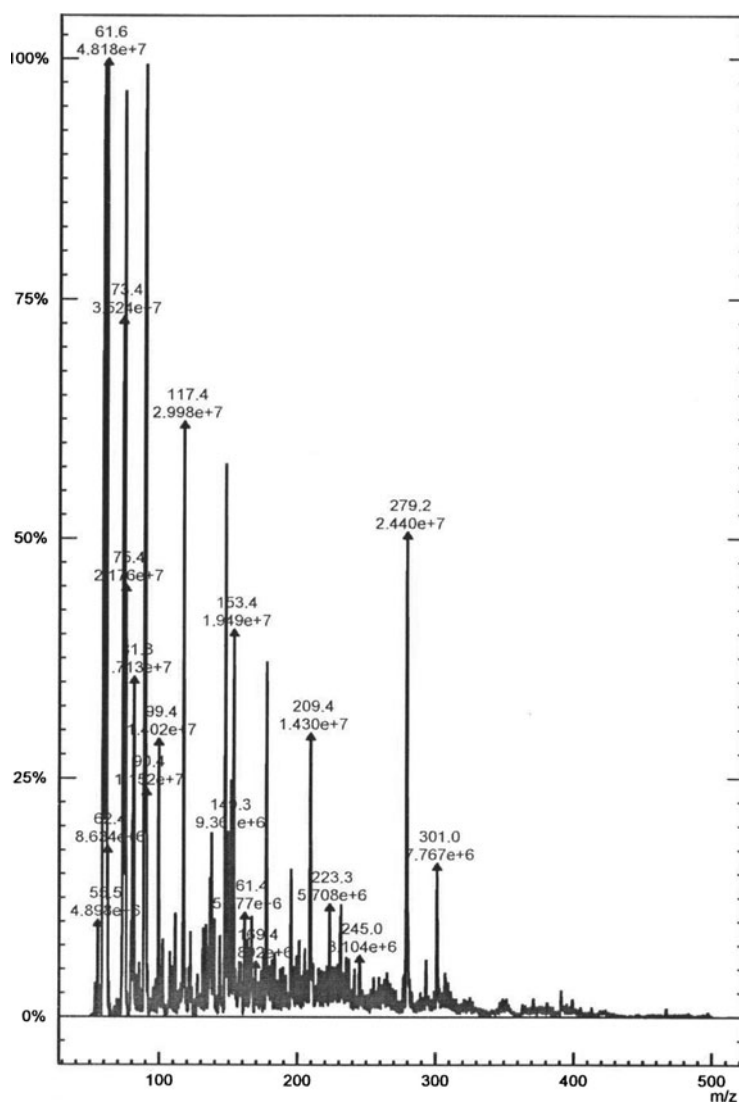
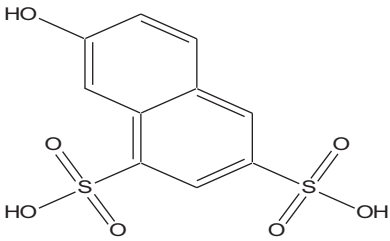
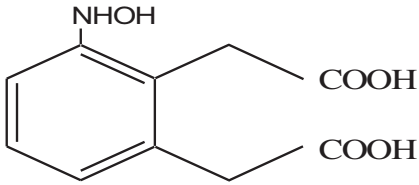
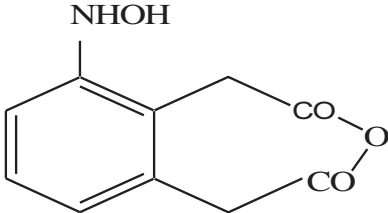
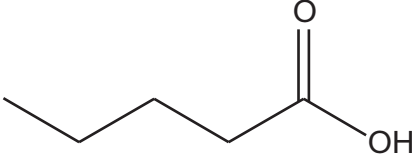
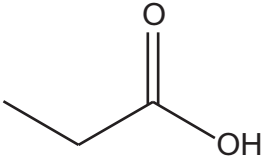
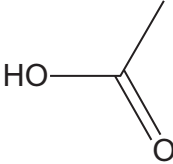


Fig. 10. LC-MS spectra of degradation products of OG.

Table 3
Proposed structures of OG degradation products

Molecular weight	Proposed structure
304	
225	7-Hydroxy naphthalene-1,3-disulphonic acid 
207	6-Hydroxyamino benzene-1,2-diethanoic acid 
102	6-Hydroxyamino benzene-1,2-diethanoic anhydride 
74	Pentanoic acid 
60	Propanoic acid 
	Ethanoic acid

steady state treatment to the concentration of complex [C] and substituting its value in Eq. (8), the following rate law has been derived:

$$\text{rate} = \frac{k_1 k_2 [\text{OG}^-] [\text{Ir}_n]_T [\text{HCF(III)}]}{k_{-1} + k_2 [\text{HCF(III)}] + k_1 [\text{OG}^-]} \quad (10)$$

The derived rate law (10) can be verified by assuming that at low concentration of HCF(III) and OG, it can be written as:

$$\text{rate} = \frac{k_1 k_2 [\text{OG}^-] [\text{Ir}_n]_T [\text{HCF(III)}]}{k_{-1}} \quad (11)$$

The derived law (11) is in agreement with the experimental results.

But at higher concentration of reactants, the rate law (10) can be written as following assuming that

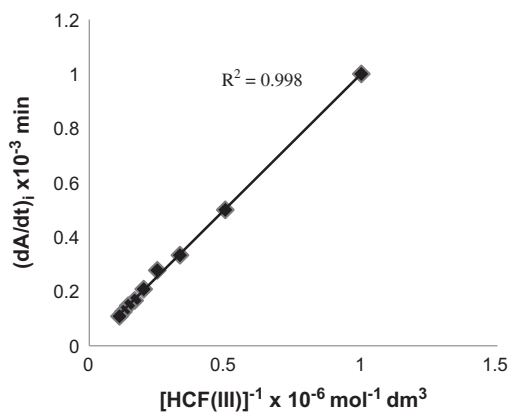


Fig. 11. Plot of rate⁻¹ vs. [HCF(III)]⁻¹.

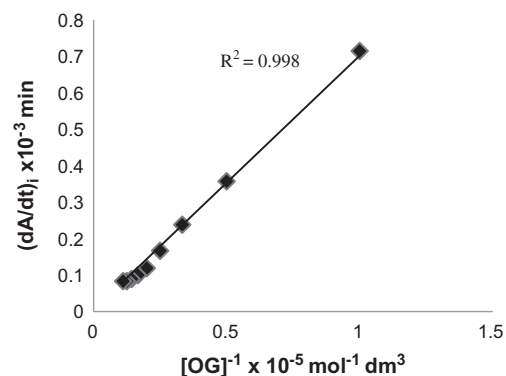


Fig. 12. Plot of rate⁻¹ vs. [OG]⁻¹.

$[\text{Ir}_n]_T$ concentration (catalyst) is very small and almost remain constant during the reaction:

$$\frac{1}{r} = \frac{k_{-1}}{k_1 k_2 [\text{OG}^-] [\text{HCF(III)}]} + \frac{1}{k_1 [\text{OG}^-]} + \frac{1}{k_2 [\text{HCF(III)}]} \quad (12)$$

The plot of $1/\text{rate}$ vs. $1/[\text{HCF(III)}]$ (Fig. 11) and $1/\text{rate}$ vs. $1/[\text{OG}]$ (Fig. 12) gives straight line. A close examination of these figures clearly indicates that these are evidently straight line with positive intercept at $1/\text{rate}$ axis showing the validity of derived rate law equation on the basis of proposed mechanism.

4. Conclusion

This study confirms the successful oxidative degradation of an azo dye, OG by HCF(III) in the presence of Ir nanoparticles. Kinetics of dye degradation showed that solution pH, $[\text{Ir nano}]$, $[\text{HCF(III)}]$ and $[\text{OG}]$ are the main factors that influence the degradation rate. The reaction follows first-order kinetics with respect to HCF(III) at optimum pH 8.0 and constant temperature of $40 \pm 0.1^\circ\text{C}$. The order of reaction with respect to $[\text{OG}]$ has been found to be one at its lower concentration tending towards zero at its higher concentration. Ir nanoparticles proved to be effective catalyst for the degradation of OG as the rate of the reaction increases with an increase in the concentration of Ir nano. The catalyzed reaction is three to four times faster than the uncatalyzed reaction. This may be due to the presence of Ir nanoparticles as catalyst which improved the reaction rate by providing larger surface area to volume ratio. Moreover, these nanoparticles can be recovered and reused making them potential candidates for dye degradation technologies. The UV-vis, FT-IR, HPLC, LC-MS of degradation product showed the formation of simpler and less hazardous compounds, 6-hydroxyamino benzene-1,2-diethanoic acid, 6-hydroxyamino benzene-1,2-diethanoic anhydride and 7-hydroxy naphthalene-1,3-disulphonic acid as minor degradation products and pentanoic acid, propanoic acid, ethanoic acid as major degradation products.

In the present method, the concentration of HCF(III) used to degrade OG is 10 times less than that of the dye concentration, while in the reported Fenton oxidation method, the concentration of oxidant is same or more than that of the dye concentration [25,26]. Thus, the present method seems to be better than other conventional methods due to its low cost, easy availability and effectiveness. About 12% degradation of OG was obtained under the studied experimental conditions in 1 h. The results of this

study can be used to design a suitable process to get higher percentage degradation of OG by increasing the concentrations of HCF(III) and Ir nanoparticles. After degradation of dye, HCF(III) converts into HCF(II) which is non-toxic and is used in food industries for metal precipitation [27].

References

- [1] S.A. Abo-Farha, Photocatalytic degradation of mono-azo and diazo dyes in wastewater on nanometer-sized TiO_2 , *Researcher* 2(7) (2010) 1–20.
- [2] J. Madhavan, F. Grieser, M. Ashokkumar, Degradation of orange-G by advanced oxidation processes, *Ultrason. Sonochem.* 17 (2010) 338–343.
- [3] V. Dulman, S.M. Cucu-Man, R.I. Olariu, R. Buhaceanu, M. Dumitraş, I. Bunia, A new heterogeneous catalytic system for decolorization and mineralization of Orange G acid dye based on hydrogen peroxide and a macroporous chelating polymer, *Dyes Pigm.* 95 (2012) 79–88.
- [4] A. Khalid, S. Mahmood, Biodegradation of azo dyes by *Actinobacteria*, *Environ. Sci. Eng.* (2015) 297–314.
- [5] X. Liu, Z. Chen, Z. Chen, M. Megharaj, R. Naidu, Remediation of Direct Black G in wastewater using kaolin-supported bimetallic Fe/Ni nanoparticles, *Chem. Eng. J.* 223 (2013) 764–771.
- [6] A.D. Bokare, R.C. Chikate, C.V. Rode, K.M. Paknikar, Iron-nickel bimetallic nanoparticles for reductive degradation of azo dye Orange G in aqueous solution, *Appl. Catal. B* 79 (2008) 270–278.
- [7] Z. Sun, Y. Chen, Q. Ke, Y. Yang, J. Yuan, Photocatalytic degradation of a cationic azo dye by TiO_2 /bentonite nanocomposite, *J. Photochem. Photobiol., A: Chem.* 149 (2002) 169–174.
- [8] K. Tanaka, K. Padermpole, T. Hisanaga, Photocatalytic degradation of commercial azo dyes, *Water Res.* 34 (2000) 327–333.
- [9] S.H. Lin, C.F. Peng, Continuous treatment of textile wastewater by combined coagulation, electrochemical oxidation and activated sludge, *Water Res.* 30 (1996) 587–592.
- [10] A. Khenifi, Z. Boubarka, H. Hamani, H. Illikti, M. Kameche, Z. Derriche, Decoloration of Orange G (OG) using electrochemical reduction, *Environ. Technol.* 33 (9) (2012) 1081–1088.
- [11] W.X. Zhang, Nanoscale iron particles for environmental remediation: An overview, *J. Nanopart. Res.* 5(3–4) (2003) 323–332.
- [12] T. Poursaberi, M. Hassanisadi, F. Nourmohammadian, Application of synthesized nanoscale zero-valent iron in the treatment of dye solution containing Basic Yellow 28, *Prog. Color Colorants Coat.* 5 (2012) 35–40.
- [13] S. Jansat, M. Gómez, K. Philippot, G. Muller, E. Guieu, C. Claver, S. Castillón, B. Chaudret, A Case for enantioselective allylic alkylation catalyzed by palladium nanoparticles, *J. Am. Chem. Soc.* 126 (2004) 1592–1593.
- [14] A. Goel, S. Sharma, A kinetic study on the oxidation of glycine by hexacyanoferrate(III) ions in presence of iridium nanoparticles, *J. Chem. Biol. Phys. Sci. Sec. A* 2(2) (2012) 628–636.

- [15] A. Goel, S. Sharma, Colloidal iridium nanoparticles in the oxidation by hexacyanoferrate(III) in alkaline medium—A kinetic study, *J. Indian Chem. Soc.* 89(4) (2012) 507–512.
- [16] A. Goel, R. Bhatt, Neetu, Kinetic studies on nanocatalysis in some oxidation reactions, *Int. J. Res. Chem. Environ.* 2(1) (2012) 210–217.
- [17] A. Goel, R. Bhatt, R. Lasyal, Kinetic and mechanistic study of the oxidation of Orange II by hexacyanoferrate(III) ions catalyzed by iridium nanoclusters, *Int. J. Chem. Sci.* 12(4) (2014) 1527–1537.
- [18] A. Goel, N. Rani, Effect of PVP, PVA and POLE surfactants on the size of iridium nanoparticles, *OJIC* 2 (2012) 67–73.
- [19] A.P. Davis, C.P. Huang, Removal of phenols from water by photocatalytic oxidation process, *Water Sci. Technol.* 21 (1989) 455–464.
- [20] A.V. Rupa, D. Manikandan, D. Divakar, T. Sivakumar, Effect of deposition of Ag on TiO₂ nanoparticles on the photodegradation of Reactive Yellow-17, *J. Hazard. Mater.* 147(3) (2007) 906–913.
- [21] S.A. Singh, G. Madras, Photocatalytic degradation with combustion synthesized WO₃-TiO₂ mixed oxides under UV and visible light, *Sep. Purif. Technol.* 105 (2013) 79–89.
- [22] A. Tripathi, S.K. Srivastava, Biodegradation of orange G by a novel isolated bacterial strain *Bacillus megaterium* ITBHU01 using response surface methodology, *Afr. J. Biotechnol.* 11(7) (2012) 1768–1781.
- [23] R.M. Silverstein, Francis X. Webster, *Spectrometric Identification of Organic Compound*, sixth ed., John Wiley & Sons, Inc., 136–138.
- [24] V.N. Daneshvar, M.H. Rasoulifard, Electro-Fenton degradation of synthetic dye mixture: Influence of intermediates, *J. Environ. Eng. Manage.* 19(5) (2009) 277–282.
- [25] S.P. Sun, C.J. Li, J.H. Sun, S.H. Shi, M.H. Fan, Q. Zhou, Decolorization of an azo dye Orange G in aqueous solution by Fenton oxidation process: Effect of system parameters and kinetic study, *J. Hazard. Mater.* 161 (2009) 1052–1057.
- [26] Y. Zhang, G. Liu, D. Li, Y. Tian, L. Zhang, L. Li, Solid super acid of S₂O₈²⁻/Fe_xO_y-CuO_x catalytic degradation of orange IV, *Adv. Mater. Res.* 239–242 (2011) 182–185.
- [27] T. Schareina, A. Zapf, M. Beller, Improving palladium-catalyzed cyanation of aryl halides: Development of state-of-art methodology using potassium hexacyanoferrate(II) as cyanating agent, *J. Organomet. Chem.* 689 (2004) 4576–4583.